

# FLOW SEPARATION

Aerodynamics  
Bridge-Pier Design  
Combustion Chambers  
Human Blood Flow  
Building Design Etc.

(Form Drag, Pressure Distribution, Forces and Moments, Heat And Mass Transfer, Vortex Shedding)



# Separation and Drag

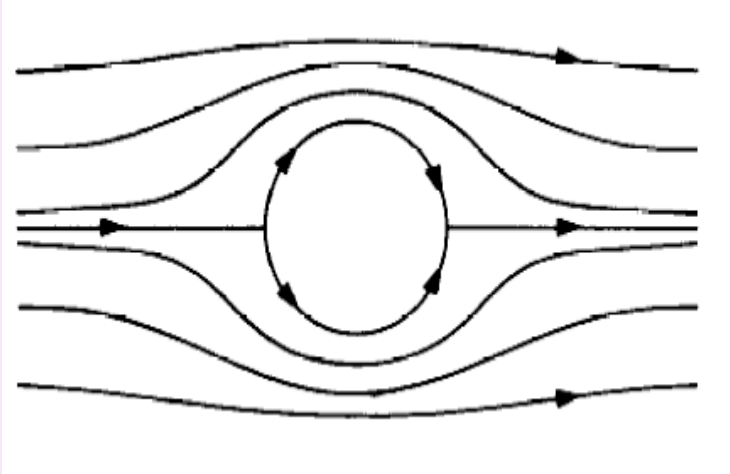
Total drag = friction drag + form drag

No separation, then friction drag dominates,  
with separation form drag dominates.

*boundary layer separation* results in a large increase in the drag on the body because of increased form drag.

# Why does separation increase the drag ?

Start from D'Alembert's paradox



Applying Bernoulli's equation to the streamline around the cylinder we find that the pressure distribution is symmetrical also so that the total pressure force on the upstream side of the cylinder is exactly equal to the pressure on the downwind side. So net force on the cylinder is zero.

If the flow of a viscous fluid about a body is such that the boundary layer remains attached, then we have almost the same result--we'll just have a small drag due to the skin friction.

However, if the boundary layer separates and the coefficient of drag is 1.2 , much larger than the coefficient of drag due to skin friction 0.01.

# Some interesting drag facts

$$D \sim \rho U^2 A / 2$$

$$P = D U = \rho U^3 A / 2$$

increases with the *cube* of the speed.

What it means is its going to take you 8 times the power to ride a bicycle at 30 mph than riding it at 15 mph.

a dimpled golf ball has one-fifth the drag of a smooth golf ball of the same size . Why ?

# 3D Separation classification by Skin-friction Topology

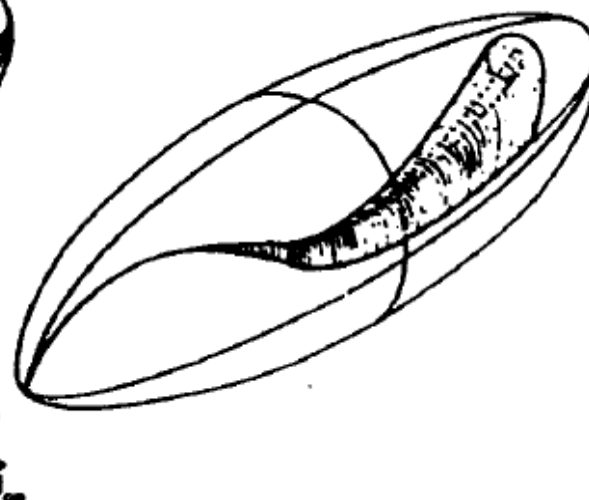
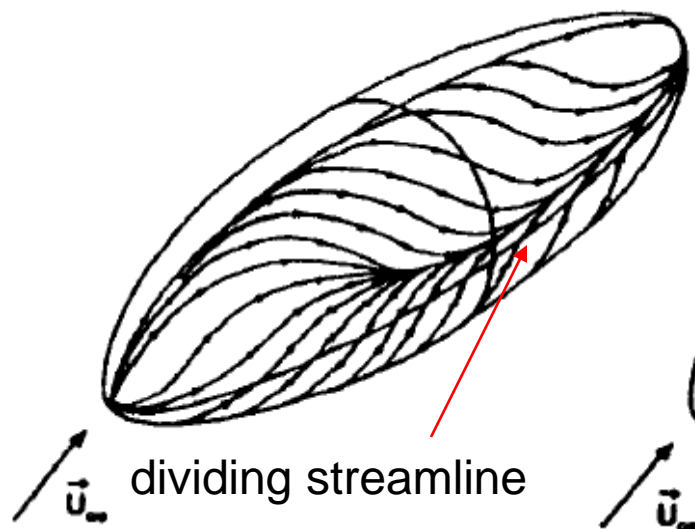
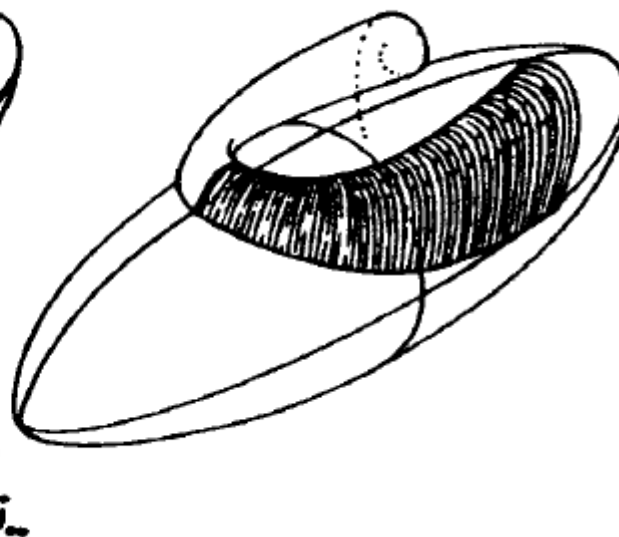
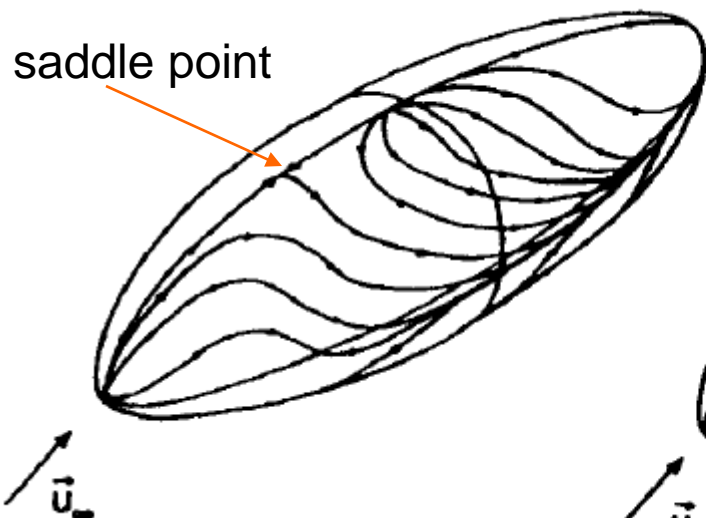
Open and Closed type separation

Open - Flow upstream of separation enters separation region. Separation occurs along a dividing streamline

Closed – Flow upstream of separation does not enter the separation region (bubble). Flow separates from a saddle point of separation.

closed

Open



# Classification based on shear layer reattachment

- **Separation without reattachment**

Interactions between opposite signed vortices shed from separation points

(e.g. Flow past cylinders, spheres, normal flat plates etc)

- **Separation with reattachment**

Interaction between vortices and the solid surface

(e.g. Flow past leading edge blunt cylinders, backward facing steps etc)

# Distinguishing features between the two kinds of classification

- Open and closed should not be confused with reattaching and non-reattaching
- All open separation is non-reattaching, but, closed separation can either be non-reattaching or reattaching, (i.e.) the separation bubble may shed or attach to the body
- Also, open and closed terminology is mainly used only for 3D separation as saddles and nodes cannot be accurately defined in 2D separation. Non-reattaching or reattaching terminology is more general in that sense.

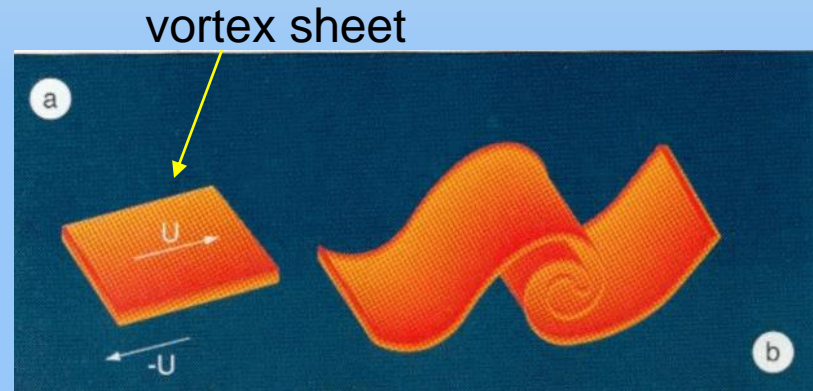
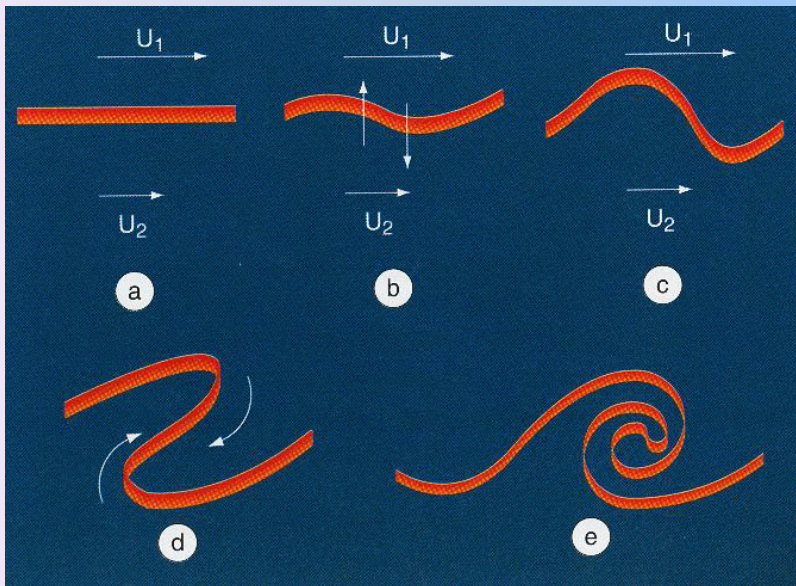


# Main instabilities in separated flows

## 1. Initial instability

**Kelvin Helmholtz instability**  
**(Both non-reattaching and reattaching)**

vortex formation due to roll up of shear layer



# Main instabilities in separated flows

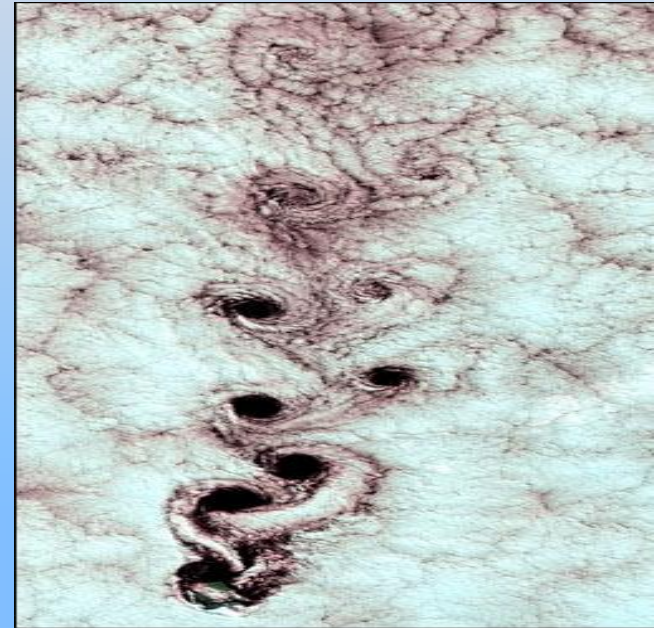
## 2. Karman instability

### **Non-reattaching**

opposite signed vortices interaction  
(asymmetric vortex shedding)

### **Reattaching**

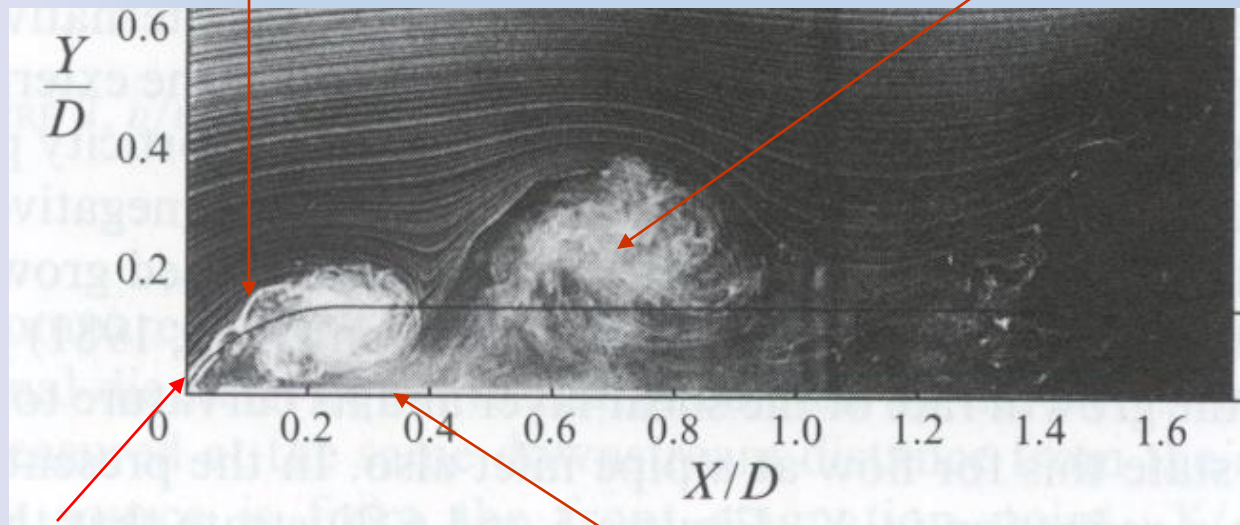
vortex and image interaction  
(symmetric vortex shedding)



# Karman type shedding in reattaching flows, illustrative example (leading edge of blunt cylinder)

KH vortices amalgamate to form large scale vortices

Karman type shedding (symmetric mode -interaction with mirror vortex)



Initial instability causes KH vortices

Large scale vortices impinge on body

# Main instabilities in separated flows

## 3. Low frequency modulation

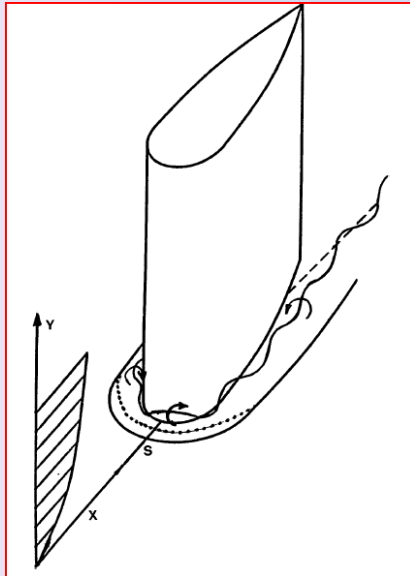
**Non reattaching** - vortex dislocations in flow past cylinders

**Reattaching** - flapping instability

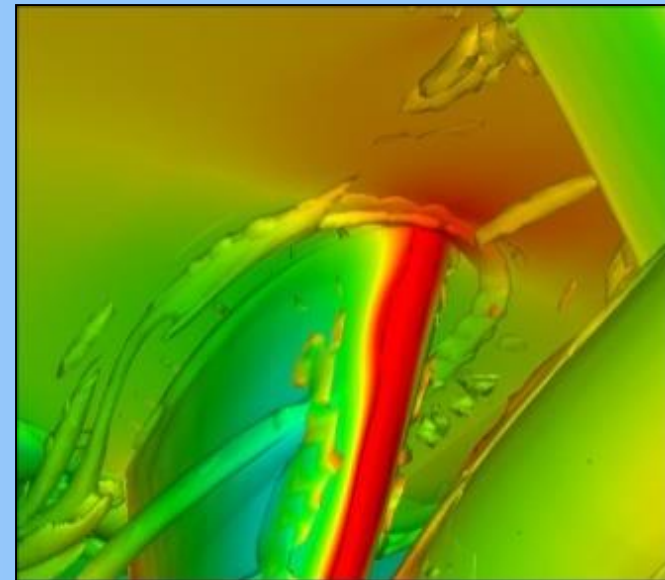
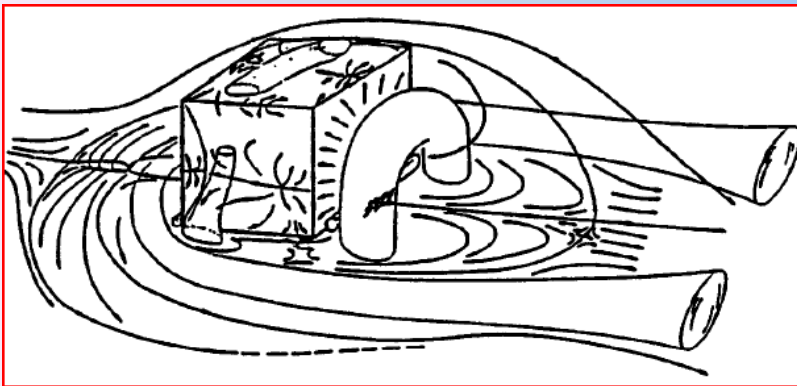
(enlarging and shrinking of separation bubble)

# Main instabilities in separated flows

## Horse shoe vortices:

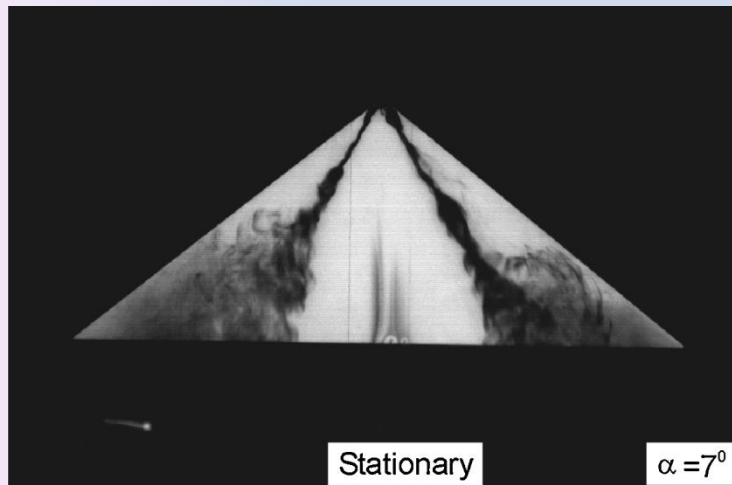


Occurs when a boundary layer encounters an obstacle attached to the surface. Presence of the obstacle causes adverse pressure gradient in the boundary layer flow, leading to three dimensional separations, i.e., horseshoe vortices that wrap around the obstacle.



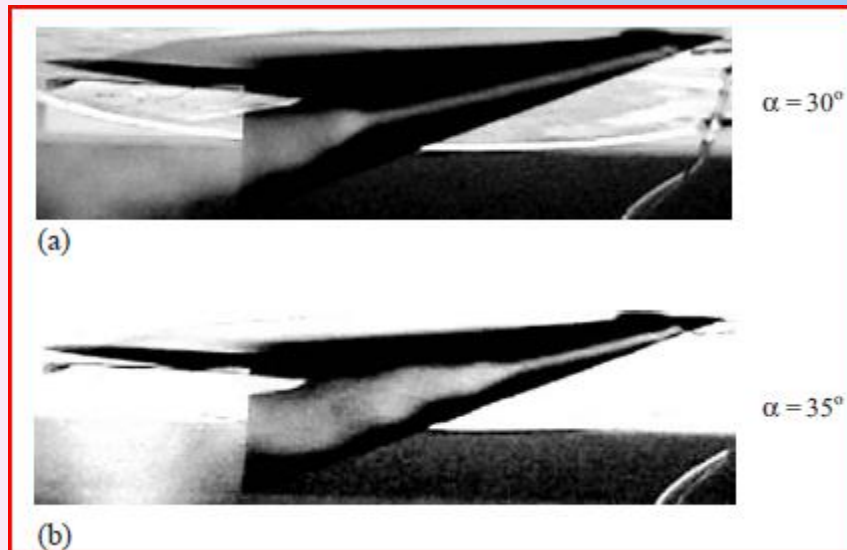
# Main instabilities in separated flows

## Helical Vortices



Boundary layer separation from the sharp leading edges of the delta wing forms three-dimensional shear layers that roll into a core of rotating vortex.

The shear layer exhibits Kelvin-Helmholtz type instability giving rise to vortical substructures which wrap around the leading-edge jet-like vortex core.



At a sufficiently high angle of attack jet-like vortices undergo a sudden expansion to a wake-like vortex.

This process is called vortex breakdown.

# The Strouhal Number

**The Strouhal Number** is a dimensionless value useful for analyzing oscillating, unsteady fluid flow dynamics problems.

The Strouhal Number can be expressed as:

$$St = \omega l / v$$

where

$St$  = Strouhal Number

$\omega$  = oscillation frequency

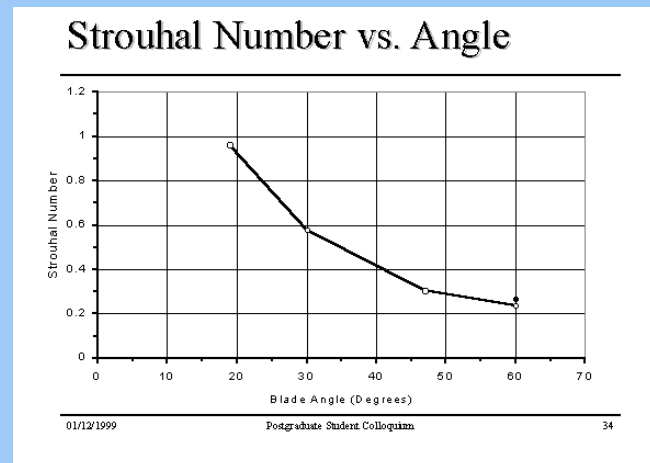
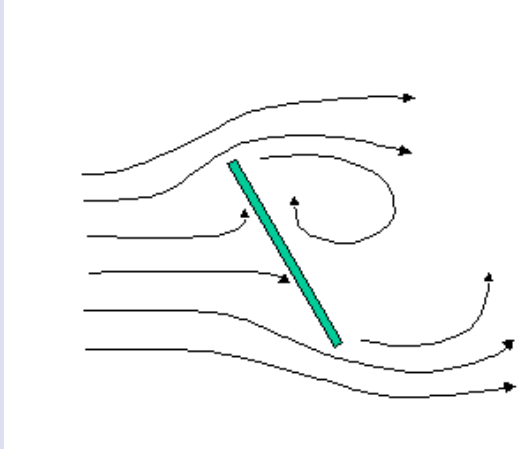
$l$  = relevant length scale

$v$  = relevant velocity scale

# General Strouhal Number

$$Sr = \frac{fD}{V}$$

where  $Sr$  is the General Strouhal number,  $f$  is the frequency of vortex shedding,  $D$  is the hydraulic diameter or length of the object in the fluid flow and  $V$  is the velocity of the fluid



Buffer the body , lower the general Strouhal number



# Relevant scales for Strouhal number

- KH instability for viscous flow

KH instability is mainly an inviscid phenomenon where vortex sheet strength (tangential velocity jump across the vortex sheet) determines the instability frequency.

Related term in viscous flows is the momentum thickness which involves  $\tau_w = \mu \delta u / \delta y$ , velocity difference across the shear layer.

Relevant velocity scaling would be the shear layer velocity.

*$St_\theta = f_{KH} \theta / U_S$  is observed to be constant throughout a range of  $Re$ , but changes with geometry.*

# Relevant scales for Strouhal number

- Karman instability.

Due to interaction between two oppositely signed vortices.

So, Relevant length scale would then be distance between the two separated shear layers.

And, velocity scaling is shear layer velocity

*$St_U = f_{KH} h / U_S = 0.08$ , found to be constant through both  $Re$  and geometry, thus termed universal Strouhal number*

# Relevant scales for Strouhal number

- Flapping instability

- change in reattachment length.

So, relevant length scale would then be mean reattachment length

And, velocity scaling is shear layer velocity

*Frequency scales with flow velocity and reattachment length ( $St_R = f_{KH} X_R / U$ )*

# Relevant scales for Strouhal number

Horse shoe vortices:

$L$  = Thickness of the body

$V$  = Boundary layer velocity

$F$  = largest frequency

Helical vortices:

Frequency x distance from  
vortex break down =  
constant

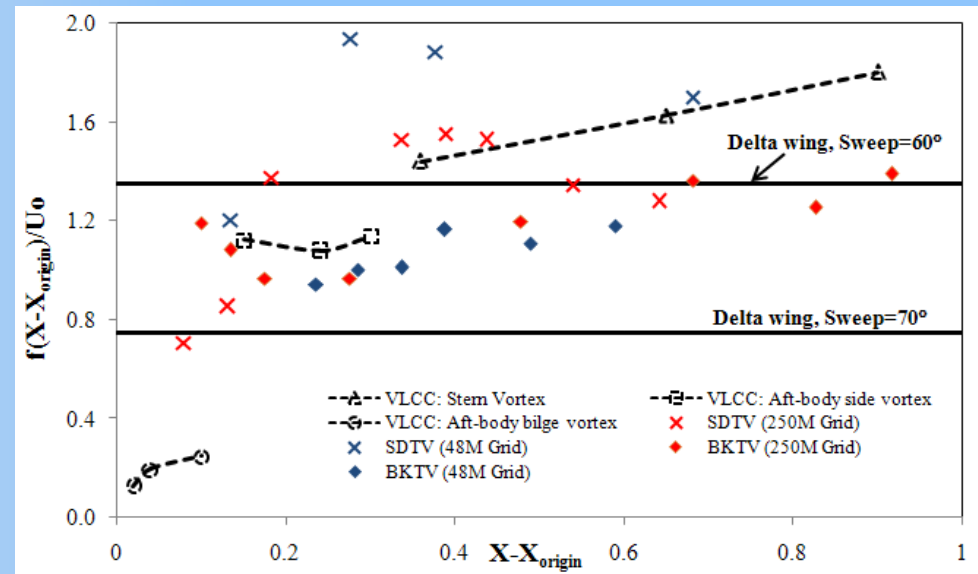
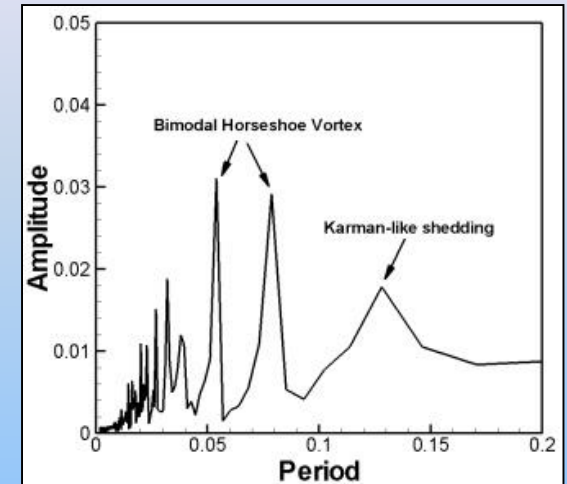





Table 1 Reattaching flows; Summary of frequencies detected

Re-attaching flows Geometry	Parameters	Regime	Separation type	High frequency (Kehrin Helmholtz instability- Scales with $\theta$ )		Medium frequency (vortex shedding, scales with $h$ )		Low frequency ( Flapping- scales with reattachment length $X_R$ )		References
				General St. No. $St_G = fH/U_\infty$	Scaled St.No. $St_s = f_{osc} \theta / U_\infty$	General St. No. $St_G = fH/U_\infty$	Universal St. No. $St_u = fh/U_\infty$	General St. No. $St_G = fH/U_\infty$	Scaled St.No. $St_s = fX_R/U_\infty$	
 Blunt cylinder	Re= 22000	Turbulent	Separated and reattaching (vortex shedding due to amalgamation of shear layer vortices, shedding due to interaction with mirror vortex)	20.6		0.065*	0.07 – 0.09	0.025 <sup>a</sup>	0.25 <sup>a</sup>  $X_R$ mean = 10.1 H 6 H < $X_R$ < 13 H	Sigurdson (1995)  Kiya and Sasaki (1985)
 Backward facing step	Re=33000	Turbulent	Separated and reattaching (vortex shedding due to amalgamation of shear layer vortices, shedding due to interaction with mirror vortex)		0.022 <sup>a</sup>	0.063	< 0.063	0.02 <sup>a</sup>  0.01358 <sup>b</sup>	0.27 <sup>a</sup>  0.18 <sup>b</sup>  $X_R$ mean= 7.4 H $X_R$ oscillates a few step heights	Lee and Sung (2002) <sup>a</sup> Eaton and Johnson (1982) <sup>b</sup> Eaton and Johnson (1980) Le et al. (1996) <sup>c</sup> Roos and Kegehan (1986)
Leading edge separation bubble of foils  		Laminar	Separated and reattaching	-	0.0068	-	Shedding same as KH shedding	Flapping observed		Pauley et al.(1990)

$h$  = half wake thickness as per Roshko's hodograph theory



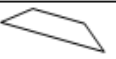


$U_s$  = shear layer velocity at separation =  $U_\infty (1 - C_{p,s})$

$U_c$  = convection velocity of shear layer = average separated shear layer velocity approximately 0.5  $U_s$

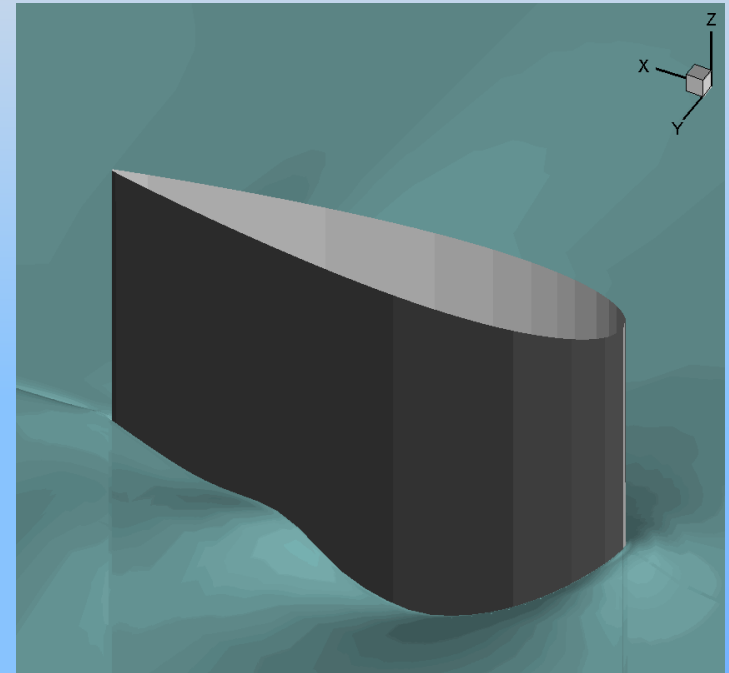
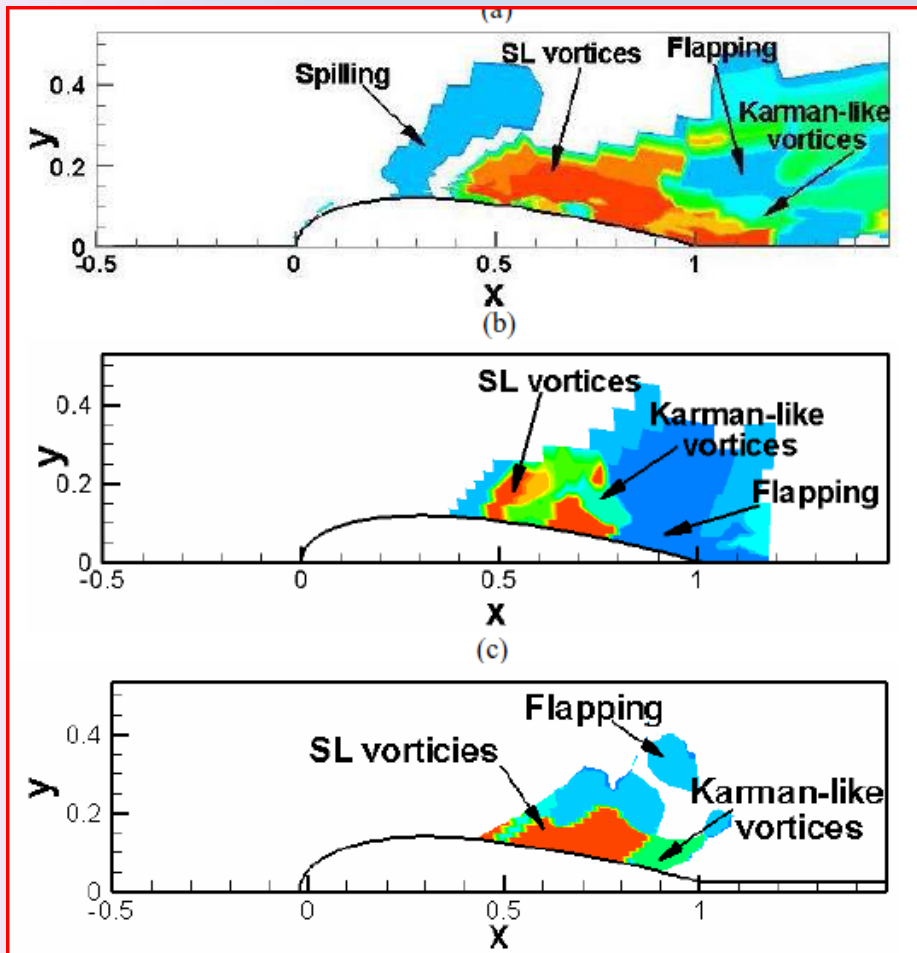
$\theta$  = momentum thickness of shear layer at separation

$\tilde{H}$  = projected length scale to flow normal direction

Table 2 Non-Reattaching flows; Summary of frequencies detected

Non-Reattaching flows Geometry	Parameters	Regime	Separation type	Low frequency modulation	Medium Frequency St.		High frequency (Kármán-Helmholtz instability)	References
					General St.No. $St_v = fH / U_\infty$	universal St. No. $St_v = fh / U_\infty$		
 Circular cylinder	$Re=49$ to 140-194	Laminar	Non reattaching, Only Spanwise vortex		0.19	0.08	$St_v = fH / U_\infty$  KH instability evident	Williamson(1996)
	190 to 260	Laminar	Spanwise / streamwise vortices Increase in formation length	Vortex dislocation low frequency due to transition from mode a to b	mode A 0.2 mode B 0.18			
	1000 to 200000	Transition, Turbulent	Decrease in formation length	Some evidence of vortex dislocation till 10000	0.2			
	10000000	Turbulent	Turbulent boundary layer separation, Shedding still observed					
 Sphere	$Re=300$ to 800	Laminar	Non reattaching helical/hairpin vortex		$\sim 0.2$	$\sim 0.08$	KH instability ( $St_v=0.2$ to 7 increasing with $Re$ )	Sakamoto and Haniu (1990)  *Kiya(2000)
	$800 < Re$ < 60000	Transition/T urbulent	Vortex tube formation due to small scale instability of separating shear layer	low frequency modulation 3 to 4 D from sphere (1/4 vortex shedding frequency*)	$\sim 0.2$	$\sim 0.08$		
	$Re > 3700000$	Turbulent	No shedding					
 Incline flat plate with bevel	$Re=20000$ $\alpha = 30$	Turbulent	Non reattaching		0.3			Chen and Fang(1996)
	$Re=20000$ $\alpha = 60$	Turbulent	"		0.2			
 Rectangular plate normal to flow	$Re= 20000$	Turbulent	Non reattaching elliptic wake with hairpin vortices	Low frequency due to axis switching	Function of aspect ratio			Kiya and Abe(1999)
 Circular disk normal to	$Re= 500$	Laminar	Non reattaching		0.1			Huang and Lin(1998)  *Kiya(2000)
	$Re= 1100$	Laminar	"		0.2			
	$Re= 1.5 \times 10^4$	Turbulent	"	Low frequency 1/3 vortex shedding frequency, pumping motion of				

# Surface Piercing NACA 0024



# Athena, $Fr = 0.25$

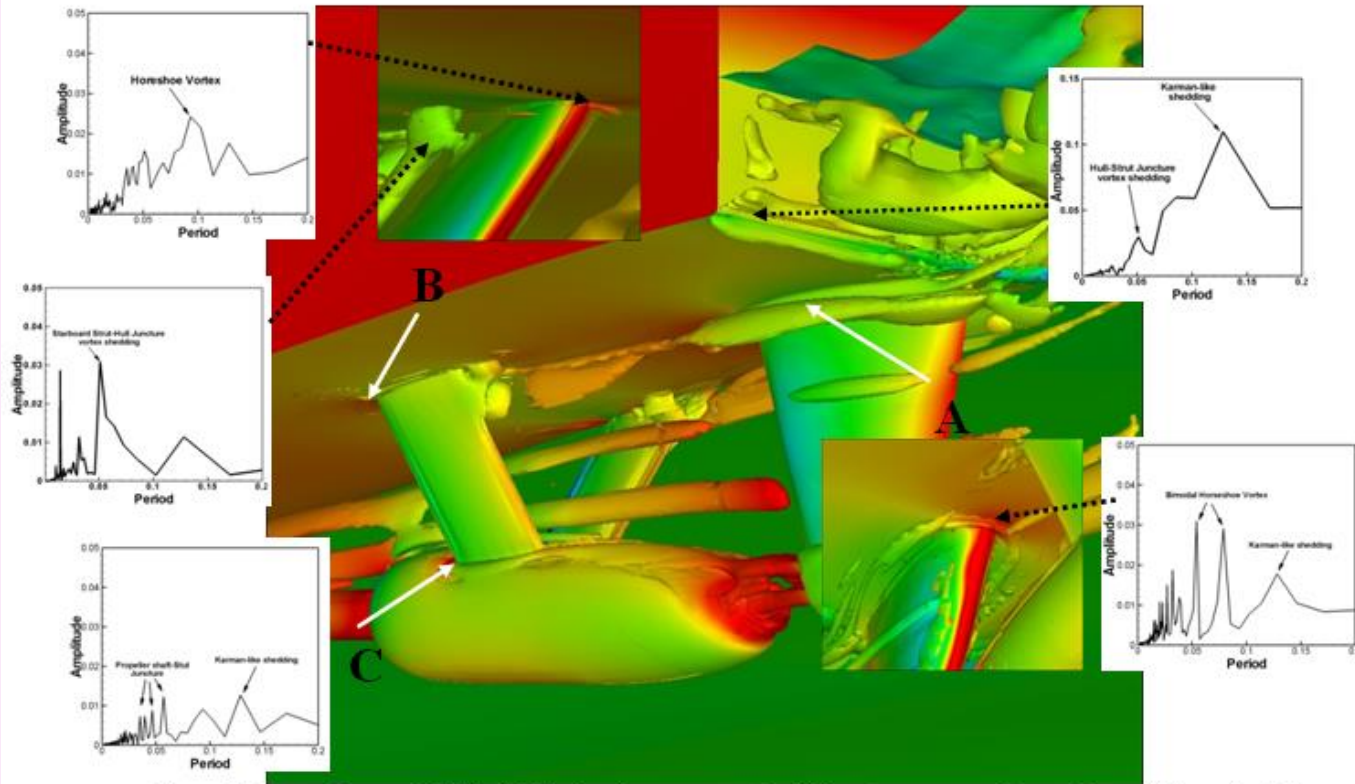
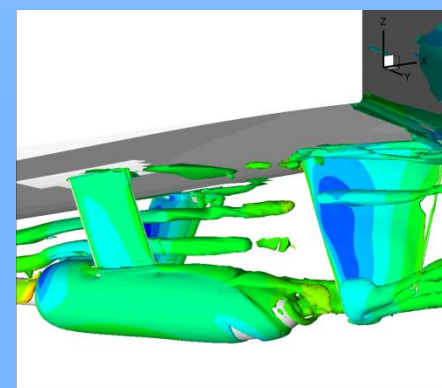
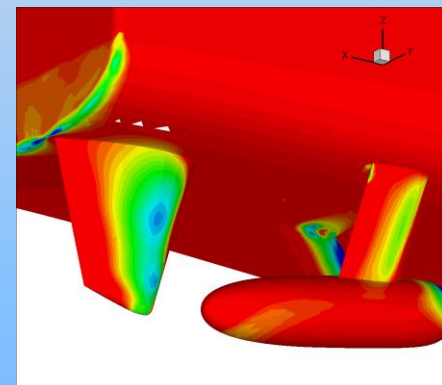
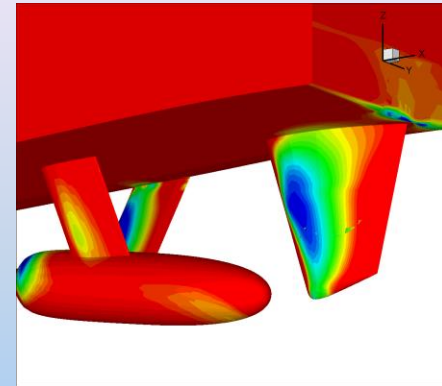


Figure 3: Iso-surfaces of  $Q_3$  ( $=300$ ) showing vortex shedding from appendages for model-scale AH simulation using DES. Three different types (A, B and C) of juncture vortices are marked and associated dominant frequency modes are shown. Contours are of the absolute pressure with levels from  $-0.5$  to  $0.1$  at an interval of  $0.02$ .





# Transom Flow Vortical Structures Instability Analysis

## Karman-like shedding

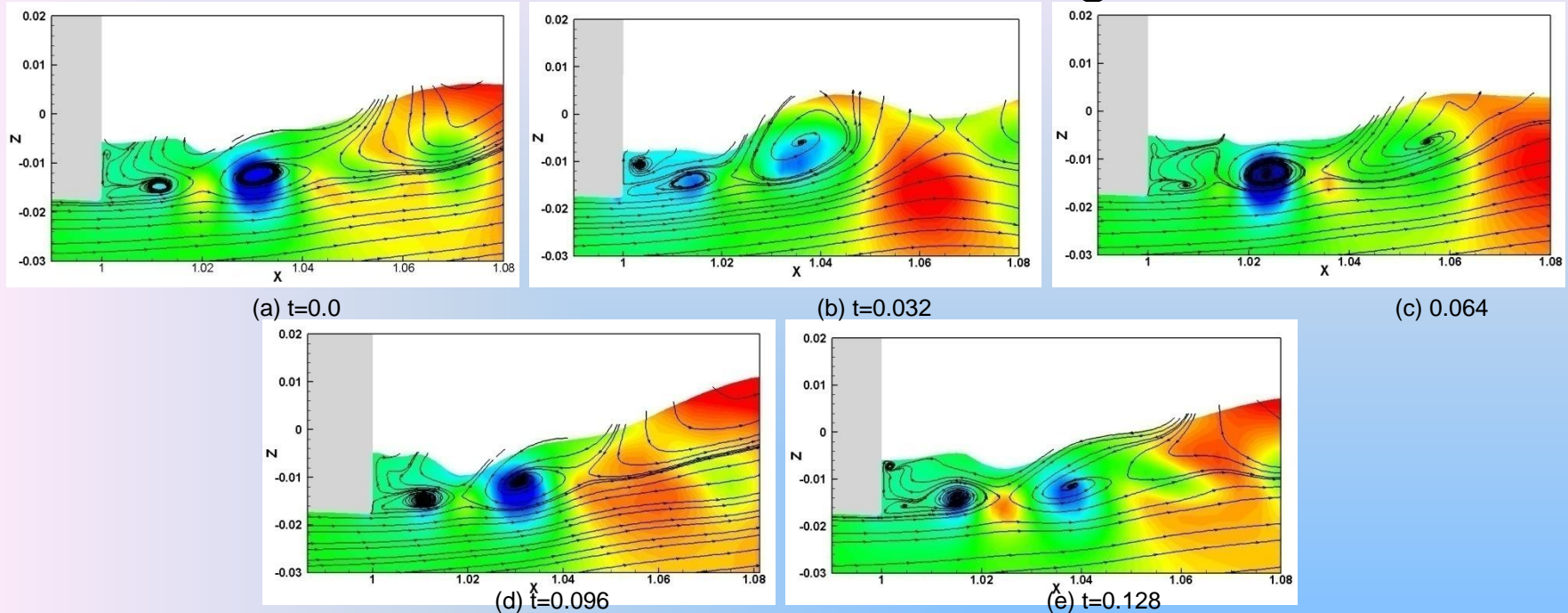


Figure : Phases of transom vortex shedding is shown for full-scale fully appended Athena, fixed sinkage and trim without propeller simulation at cross-section close to the symmetry plane  $Y=0.01$ . Contours are of the absolute pressure with levels from -0.2 to 0.1 at an interval of 0.006.

# Transom Flow Vortical Structures Instability Analysis

## Shear-layer Instability

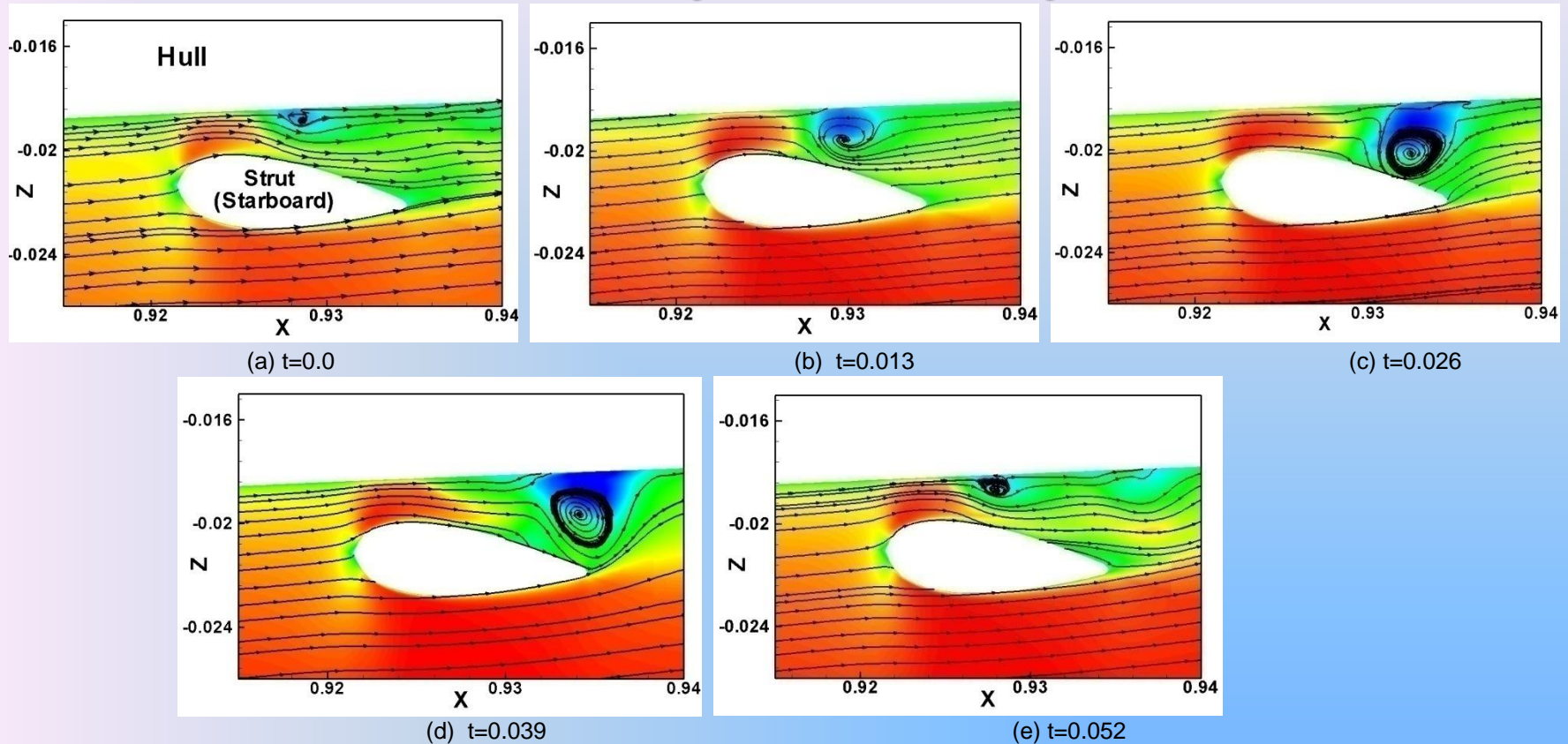


Figure: Phases of hull-strut juncture vortex shedding due to shear-layer instability is shown for full-scale, fixed motions without propeller simulation at cross-section  $Y=0.0524$  for full-scale fully appended Athena simulations.

# Transom Flow Vortical Structures Instability Analysis

## Flapping-like Instability

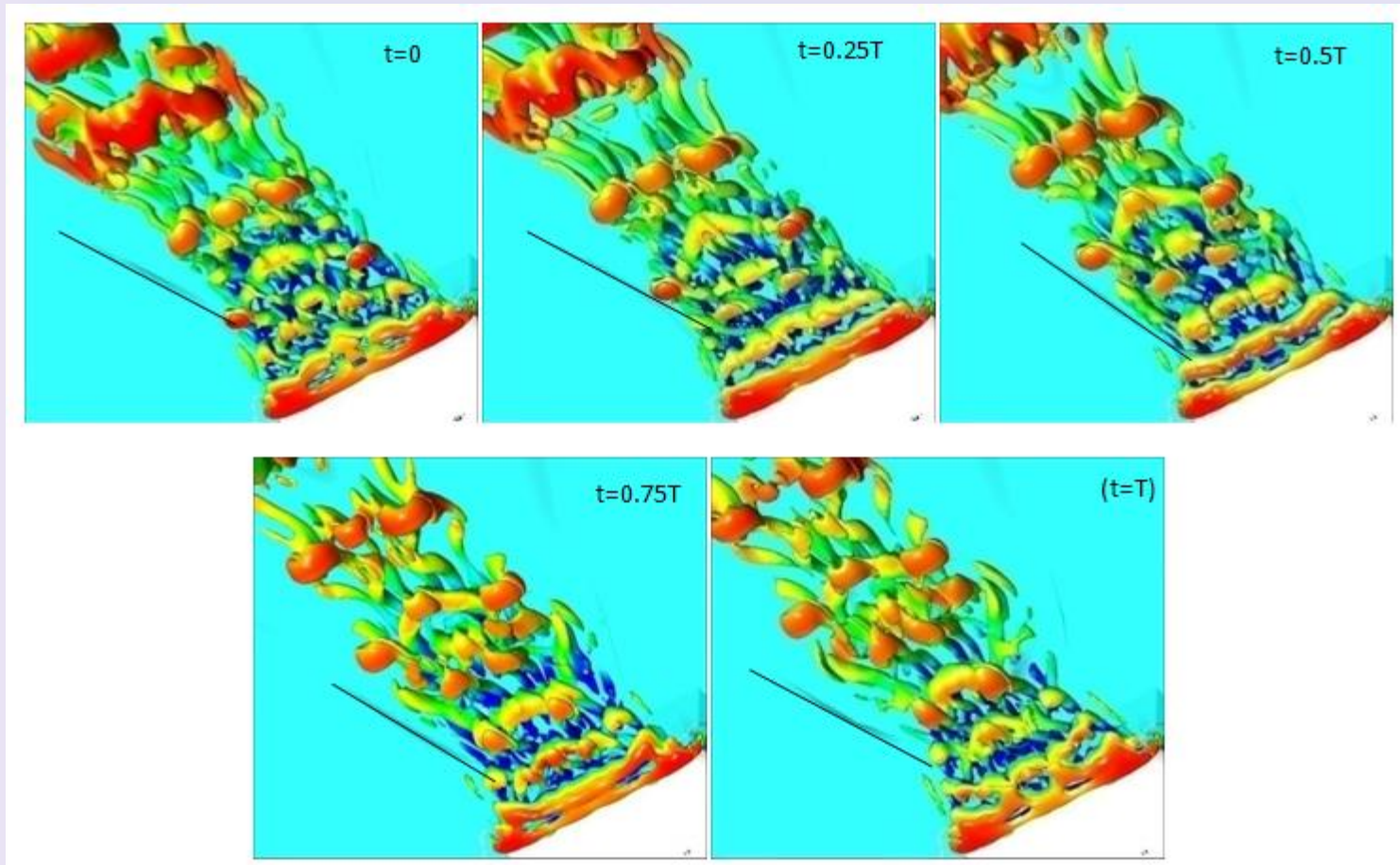
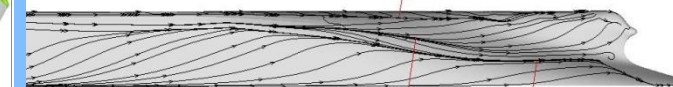
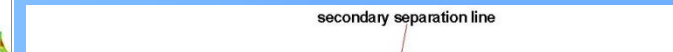
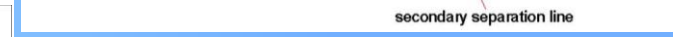
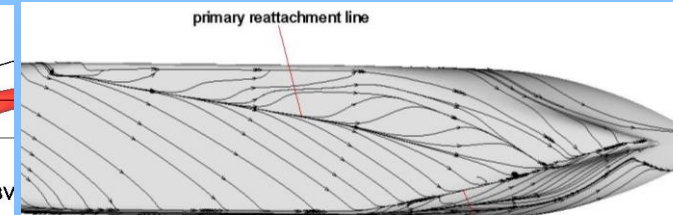
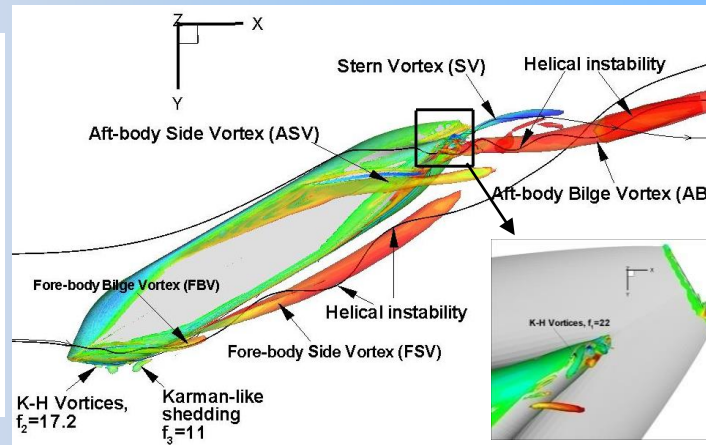
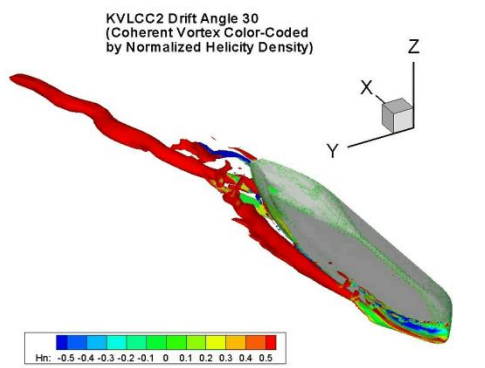
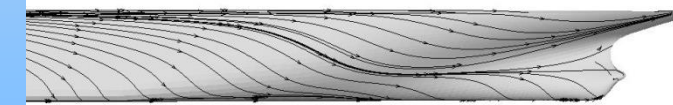
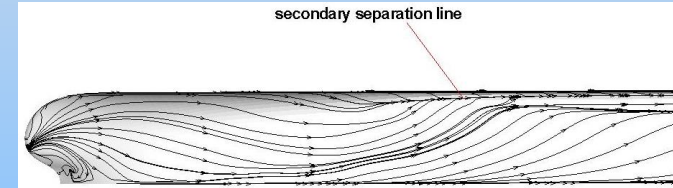
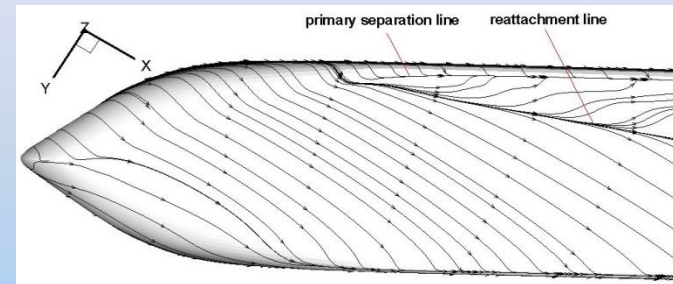
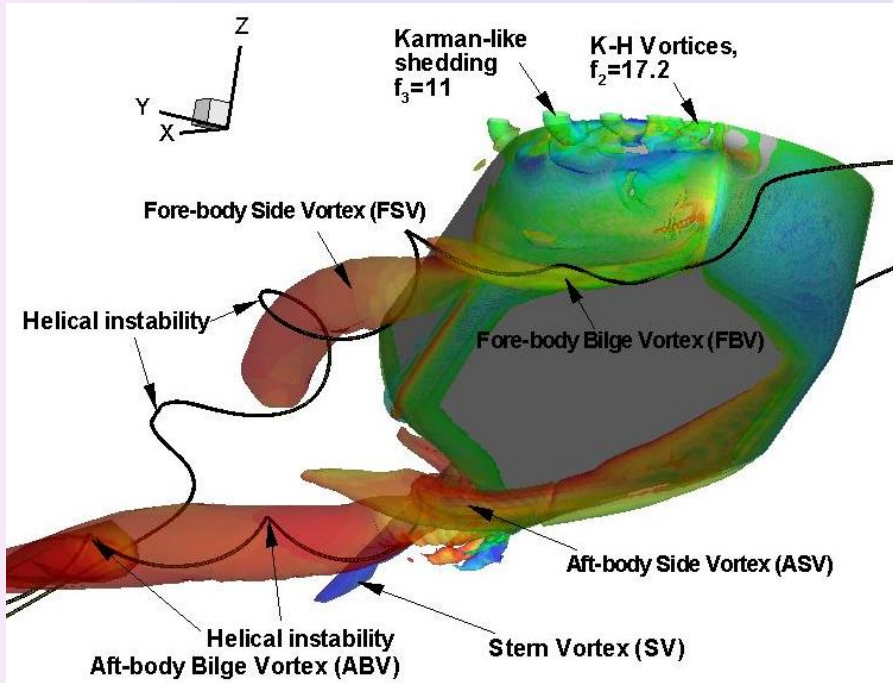


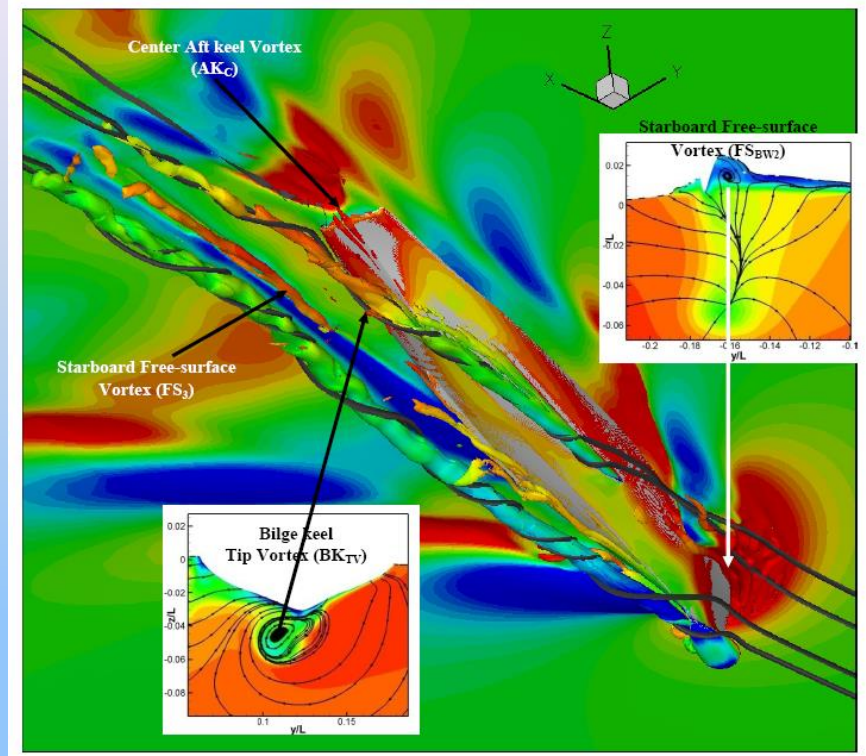
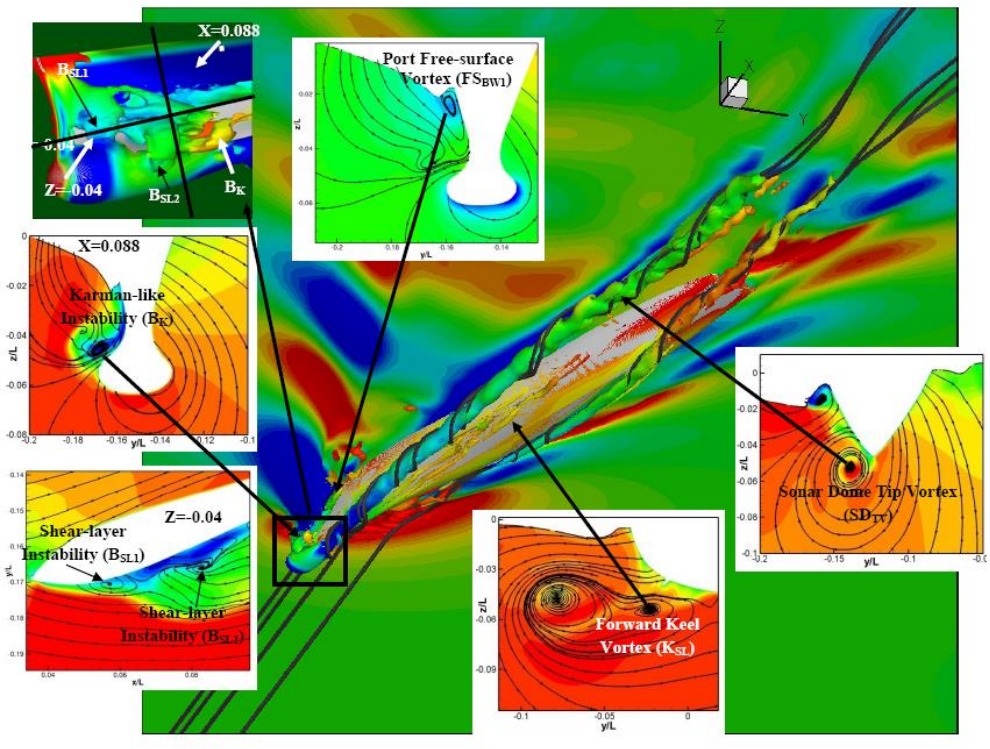
Figure: Flapping-like instability ( $\tau=0.16$ ) for DES for model-scale Athena bare hull. The vortical structures are shown by the isosurfaces of Q3 ( $=300$ ) and colored by absolute pressure with levels from -0.5 to 0.1 at an interval of 0.02.

# KVLCC2 drift angle 30° (vortex system, limiting streamlines)



Limiting streamlines

# DTMB 5415 at $\beta=20^\circ$ V4 DES Computation



- The sonar dome ( $SD_{TV}$ ) and bilge keel ( $BK_{TV}$ ) vortices exhibits helical instability breakdown.
- Shear-layer instabilities: port bow ( $B_{SL1}$ ,  $B_{SL2}$ ) and fore-body keel ( $K_{SL}$ ).
- Karman-like instabilities on port side bow ( $B_K$ ) .
- Wave breaking vortices on port ( $FS_{BW1}$ ) and starboard ( $FS_{BW2}$ ). Latter exhibits horse shoe type instability.

